STUDY OF SUBMARINE GROUNDWATER DISCHARGE ON THE WEST SHORE OF FORGE RIVER USING ELECTRICAL RESISTIVITY MEASUREMENTS AND SEEPAGE METERS

J. Durand[1], J. Wanlass[2], N. Stark[1], R. Paulsen[2], T-f. Wong[1]
[1]Department of Geosciences, State University of New York, Stony Brook, NY 11794-2100
[2]Suffolk County Department of Health Services, Bureau of Water Resources, 220 Rabro Dr., East Happauge, NY 11788

Abstract

The Forge River, (Long Island, NY) has experienced chronic hypoxia due to an excess input of nitrogen. Submarine Groundwater Discharge (SGD) is commonly recognized as a significant part of the water cycle. SGD can represent an important path for chemical substances and/or even reach up to 40% of the river-water flux to the ocean. It has thus been suggested that SGD could be one important source of nitrogen. The main challenge of studying SGD arises from its highly diffuse and heterogeneous character. Many different techniques have been developed so as to quantify and map the extent of SGD at various scales. The results of three complementary methods are presented here. Seepage meters present the advantage of giving direct measurements of the seepage rate. These measurements can be completed by both electrical resistivity profiles, which give more insight into its spatial distribution, and punctual resistivity measurements to check the profile results. The data demonstrate the existence of a significant plume of fresh water on the West shore of the river and is correlated with SGD rate close to 39cm/d. The plume extends for at least 30m towards the center of the river and is at least 7m thick close to the bank and 4m thick farther. The study of data from Forge River also shows how sensitive the inversion of the electrical resistivity data is to the water depth. It is thus critical to adapt both the data acquisition and the inversion process to take this constraint into account. Using the EarthImager2D from AGI software, we have the possibility not to fix the seawater resistivity which stabilizes the inversion and improves drastically the reliability of the results. By acquiring the data from the different methods simultaneously it will bring more constraint on the inversion and yields more reliable and accurate results.

1 Site Description

The Forge River is located between the hamlets of Moriches and Mastic in the southwestern portion of Suffolk County in New York State (Figure 1). A major tributary of Moriches Bay on the south shore of Long Island and an important and productive natural resource for both commercial and recreational users for many decades, Forge River has since 2005 experienced chronic hypoxia due to excessive nitrogen input from a number of natural and anthropogenic sources, including storm water discharges, submarine discharges that contain effluent from unsewered high-density residential housing, and wastewater from a commercial duck farm upstream. The most alarming was a fish-kill during the summer of 2006, which increased the concern about a general decline in its state of health and consequently Forge River was added to the 2006 New York State 303(d) List of Impaired Water Bodies.

Management and ecological restoration of the Forge River watershed hinge upon a comprehensive understanding of where and how nutrient loading is occurring. As is typical of Long Island streams, a significant portion of the freshwater flow of Forge River derives from groundwater, which may transport a disproportionate concentration of nutrients from the underground aquifer by submarine groundwater discharge (SGD). In a recent study of benthic fluxes of Forge River, [*Aller*, 2009] observed that the groundwater fluxes are relatively high, representing up to 73% of the total external supply of nitrogen. As this flux is largest on the more densely populated western side of the Forge watershed, it has probably contributed to the greater hypoxia and nitrogen, as well as lower oxygen levels observed in the tributaries and shorelines along the western portions of the Forge River.

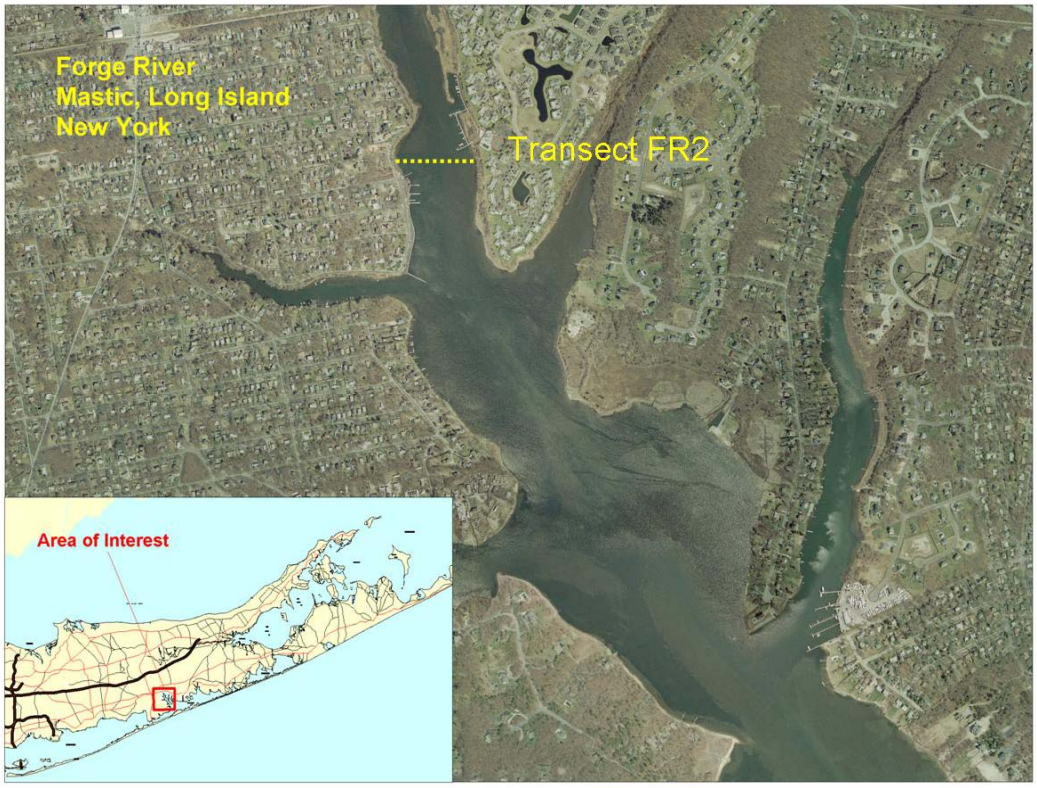

Figure 1: Forge River location and position of the transect FR2

In relation to this issue, it is important to characterize the SGD and its spatial distribution along the Forge River. In addition, SGD is expected to vary over time, especially in connection with the tidal cycles. The tidal portion of Forge River is approximately three miles long, encompassing four branches off its main stem on the west side and two on the east side. Tidal loading can exert significant influence over the encroachment of saltwater from the ocean that is counteracted by underground underflow driven by the hydraulic gradient of the aquifer. The temporal evolution of SGD is such that its peak occurs near low tide and vice versa [*R.J. Paulsen et al.*, 2001]; [*Taniguchi*, 2002].

A study was undertaken to determine the spatial and temporal distribution of SGD at selected sites along Forge River, using a multidisciplinary approach employing three complementary techniques. Here, we focus on data acquired at a selected site (transect A of the profile FR2 in Figure 1 and Figure 2) to underscore the coupling between SGD and tidal loading. The first approach we used is the direct measurement of seepage by an ultrasonic meter developed by [*R.J. Paulsen et al.*, 2001], which has the capability to measure both positive and reverse SGD with a resolution of 0.1 μm/s (0.086 cm/d). It can readily capture the evolution of SGD in response to tidal loading, and is robust enough for deployment in the field for over one month [*R. J. Paulsen et al.*, 2004].

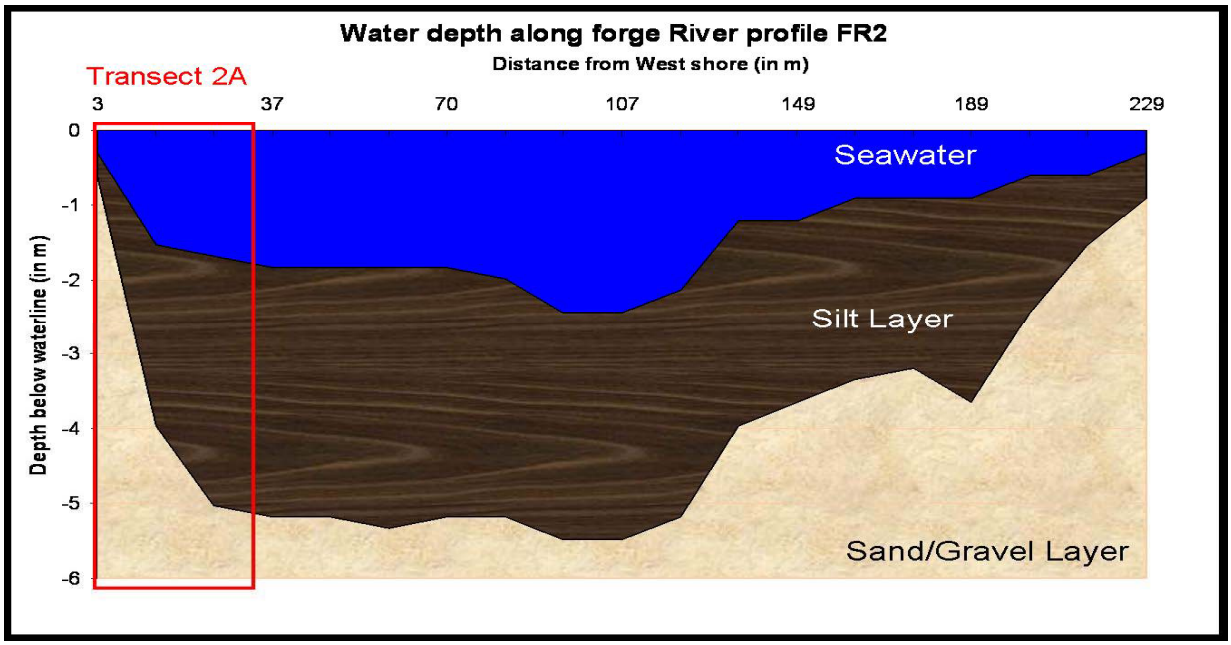

Figure 2: Water depth profile and muck layer of the transect FR2. The red rectangle indicates the position of the profile FR2A.

Although the ultrasonic seepage meter provides data of high quality, it has an intrinsic limitation in that the spatial coverage is localized and it cannot conveniently map out the spatial heterogeneity of SGD. In recent years there has been an increased use of electrical resistivity methods in hydrogeologic investigations, since they can provide extensive spatial coverage and in the context of a coastal setting, the electrical resistivity of the sediments provides a proxy for SGD [*Day-Lewis et al.*, 2006]. In our second technique, electrical resistivity data were acquired by a linear array on the sediment surface, which would be inverted to derive the 2-dimensional resistivity profile of a vertical cross-section. Since the electrical resistivity of a porous medium is primarily controlled by its porosity and the electrical resistivity of the electrolyte in the pore space [*Telford et al.*, 1990], the inferred electrical resistivity can be related to the electrolyte resistivity if the sediment porosity is relatively uniform in the section. In particular, a relatively high electrical resistivity would imply a relatively low salinity, probably due to the influx of SGD [*P. W. Swarzenski et al.*, 2007]. Repeated measurements during a tidal cycle can be inverted to infer the temporal evolution of SGD related to tidal fluctuation.

Since the interpretation of electrical resistivity data depends solely on inversion of surface measurements, it is important to validate the inferred values by conducting direct measurements of conductivity at depth. In this study this is achieved by our third approach using the Trident probe [*Chadwick et al.*, 2003], which measures the bulk electrical conductivity and subsurface temperature at selected locations. From the study of the transect FR2A we will show how important it is to take the tidal stage into account to get reliable results and also to allow sound comparisons with other methods of measurements.

2 Data Acquisition

2.1 Supersting resistivity array and EarthImage2D inversion

Stationary DC resistivity surveys were conducted using an Advanced Geosciences Inc. (AGI) *SuperSting* 8-channel receiver, interfaced to a 112' cable with 56 electrodes at a spacing of 60 cm (2 ft). With the cable resting on top of the sediment, electrical resistivity was measured by distributed dipole-dipole and Schlumberger arrays. The apparent resistivity data were processed with AGI's EarthImager 2D inversion and modeling software, using a pseudosection of the apparent resistivities as a starting model and constrained by an underwater terrain file that allows one to assign the resistivity value of all grid points above the set cable depth at all iterations. It would take ~47 minutes to complete the data acquisition process.

2.2 Trident probe

The *Trident* Probe integrates a temperature probe, an electrical conductivity probe, and a water sampler [*Chadwick et al.*, 2003]. A push-pole is used to drive this assembly into the sediment to a selected depth. The head of the push-pole is fitted with a GPS unit with WAAS capability. Data are fed to a logger, which provides real-time measurement of the temperature and conductivity of the porous sediment as functions the spatial coordinates. Utilizing a Wenner-type configuration, the electrical conductivity probe measures the conductivity of the porous medium saturated with fluid in a volume that encloses the electrode array.

In this study all the Trident measurements were made after the probes had been inserted to a depth of 45 cm below the sediment surface using the push-pole system. If strong resistance was encountered at a depth shallower than the target depth due to geological conditions or other obstructions, the station would be relocated laterally by a distance of ~30-40 cm and the push repeated. There were also instances when the sediments were so silty that the pumping system was unable to extract water samples. In these cases the station was relocated by a lateral distance of approximately 90-120 cm and the push repeated.

2.3 Ultrasonic seepage meter

Sites identified by the Trident data to have anomalously low temperature and electrical conductivity (possibly related to appreciable SGD) were selected for deployment of the seepage meter. The ultrasonic meter houses two piezoelectric transducers mounted at opposite ends of a cylindrical flow tube. Groundwater flow is captured and directed through a stainless steel funnel with a square cross section of 0.21

m^2 that is inserted approximately 10 cm into the sediment and connected to the ultrasonic device by Tygon tubing. If fluid is flowing in the tube, then travel time for the upstream propagation of sound waves against the flow direction is prolonged relative to that for downstream propagation. Our ultrasonic seepage meter is able to measure positive and reverse SGD at rates as low as 0.1 μm/sec [*R.J. Paulsen et al.*, 2001]. For this study the measurement duration was up to 24 hours, a period long enough to ensure an accurate estimation of the temporal variations[*Taniguchi et al.*, 2003].

3 Electrical Resistivity Data Processing

Electrical resistivity is a measure of how strongly a material opposes the flow of electric current. In a porous medium saturated by a fluid, the resistivity is primarily controlled by the resistivity of the electrolyte and porosity. As freshwater and seawater have different electrolyte contents, it is possible to study their relative distribution by mapping the spatial distribution of electrical resistivity of the ground. This is done by inversion of the apparent resistivity data measured at the sediment surface. A model is created using the geometrical configuration of the system and specified boundary conditions. In the case of underlying water system, it is necessary to specify the water depth along the profile with an "underwater terrain file". The model is then compared with the measurements and modified iteratively to minimize the difference between the two, characterized by a residual such as the root mean square or normalized Euclidian norm (L2). In this study the inversion was performed using AGI software EarthImager2D. This method is known to provide valuable information about the extent on SGD[*P. W. Swarzenski et al.*, 2006],[*P.W. Swarzenski and Izbicki*, 2009].

Although the use of three complementary techniques can provide useful insights into the spatial and temporal development of SGD, we also encountered significant logistical challenges in that each technique by itself is quite involving, rendering it very difficult to simultaneously undertake all three types of measurements at the same location. Furthermore the duration for acquiring a complete set of measurement of electrical resistivity may be so long that the boundary condition associated with tidal loading cannot be approximated as constant, thus complicating interpretation of the inversion results. In this pilot study, a decision was made to conduct the different types of measurements at different time, with the expectation that this may introduce uncertainties in connection with variability in the tidal stage relative to bathymetry. We will first discuss some of our attempts to address this issue, as well as the lessons we have learned from this analysis, which will guide us in future coordinated efforts to simultaneously acquire the necessary data.

3.1 Effect of the water depth on the inversion

For inversion of the resistivity data, the simplest approach is to fix the surface water resistivity at a constant value, which we took to be 0.285 ohm-m, the average sea water resistivity measured at our location. This is illustrated with a set of data we acquired on August 16, 2007 near high tide. The bathymetry (Figure 2) was measured on October 25, 2007 at ~12 pm, which was half time from high tide towards low tide. To investigate the sensitivity of the inverted profiles to variation in tidal stage, we used the same set of resistivity data but with two different underwater terrain files. The first one corresponds to the water depth measured. For the second one, 50 cm of water was added,

corresponding to the maximum variation due to tide amplitude for the day of acquisition. In this sense, the two inverted profiles would bracket the various scenarios that fall between these end-members.

The two profiles (Figure 3) show features typical of inversion results we obtained when we constrained the surface water resistivity to be uniform. First, the residuals were very high, an indication of significant error associated with the estimated parameters in the optimized model. In Figures 3a and 3b, the RMS errors were 26.5% and 24.9%, respectively. Second, the profiles show numerous small plumes, but such geometric complexity may represent numerical artifacts and it seems unlikely that the resistivity measurement can resolve such refined features or even reach values as high as 100,000 ohm-m.

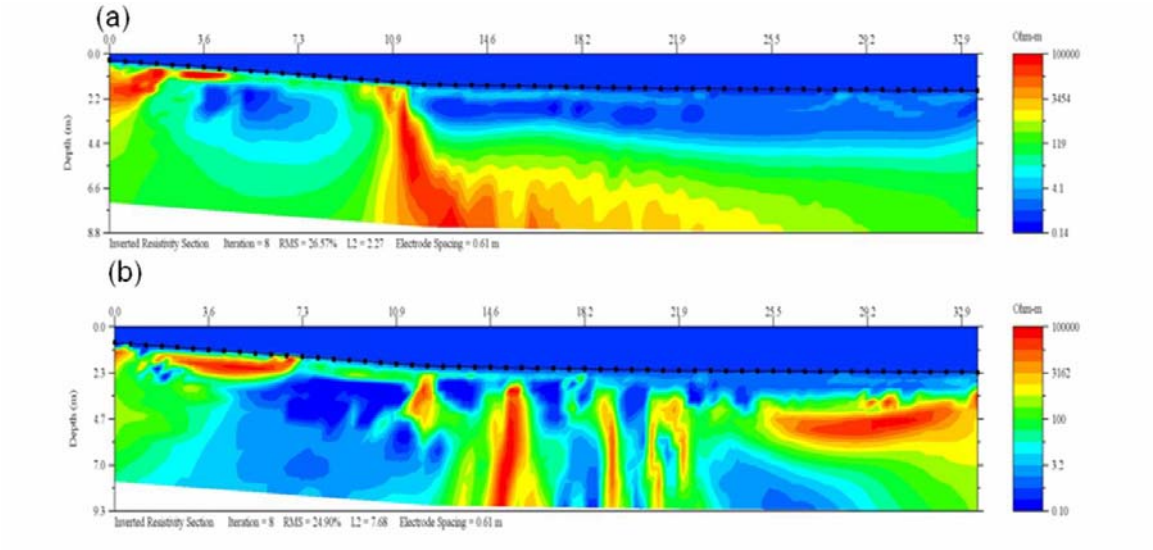

Figure 3: Water depth effect on the inversion of the transect FR2A.
West shore of Forge River, 08/16/2007 at high tide. (a): Original water depth. (b): Increase of the water depth about 50cm, maximum tide amplitude variation of that day.

3.2 Effect of surface water resistivity

After repeated trials with different approaches, we were able to obtain significant improvement in our inversion results by relaxing the constraint of uniform resistivity in the body of water overlying the formation. This is illustrated in Figure 4b, in which the resistivity of only the grid points on the free surface was fixed (at 0.285 ohm-m), with the consequence that resistivity of the water could vary spatially, possibly due to the influx of SGD from the bottom. After we relaxed the boundary condition, the model converged more quickly, and the RMS residual decreased significantly to a relative low value of 4%. Similarly the L2 residual decreased from a very high value of 2.27 (Figure 4a) to 0.59 (Figure 4b). In the inverted profiles obtained by two different approaches, the plumes of relatively high resistivity (as proxy for SGD) are qualitatively similar, with one spreading laterally near the shore and a second further away from shore that seems to propagate subvertically. However, the spatial extents of the plumes in Figure 4b are larger. It should also be noted that the color scales for resistivity are different in the two figures. The more spatially disperse plumes in Figure 4b are inferred to have lower resistivity.

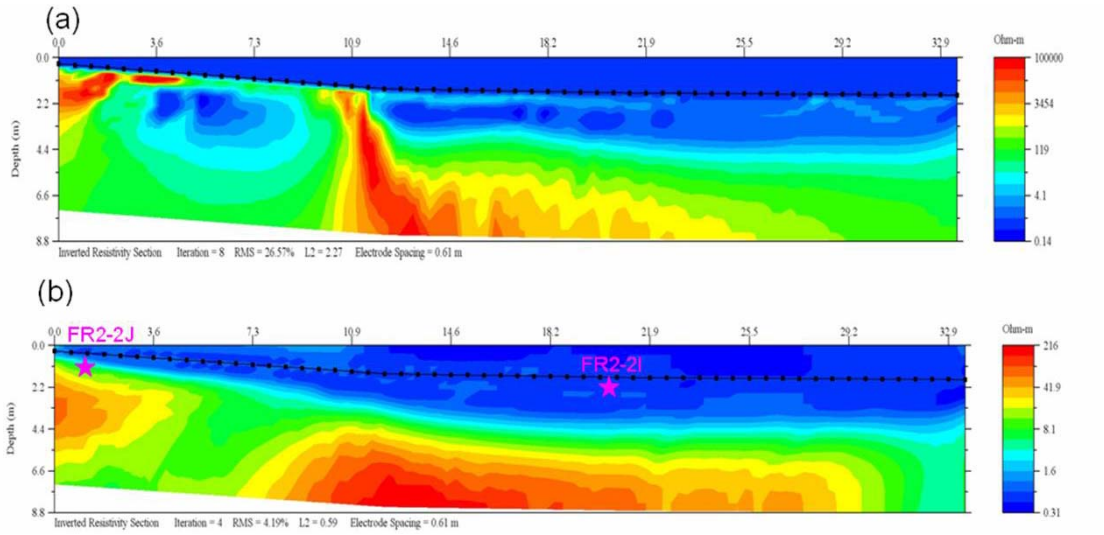

Figure 4: Water resistivity effect on the inversion of the transect FR2A.
(a): Water resistivity value fixed at 0.285 Ohm.m. (b) Water resistivity let unknown and calculated by inversion. The stars indicate the position of the Trident probe measurements.

3.3 Effect of tidal loading

We present in Figure 5 inverted resistivity profiles derived from two sets of data acquired on December 8, 2008 near high and low tides. The inversion was done using an approach identical to that for Figure 4b, fixing the resistivity of sea water at the free surface only. The residuals (5.41% and 3.69%) were relatively low, and we have used identical color codes for the resistivity. Although the data were acquired at dates separated by more than a year, the two plumes of relatively high resistivity mapped out in Figures 5a, 5b and 4b are qualitatively similar, with the implication that this is a robust feature in spite of seasonal and tidal effects. Overall the resistivity of the near-shore plume in Figure 4b seems somewhat lower than that in Figures 5a and 5b, which can be partly attributed to temperature being higher in August than in December.

Comparison of the two profiles in Figures 5a and 5b underscores the significant influence of tidal loading on the spatial distribution of electrical resistivity, indicating that SGD tends to spread towards the sea during a tidal cycle in the transition from high tide to low tide.

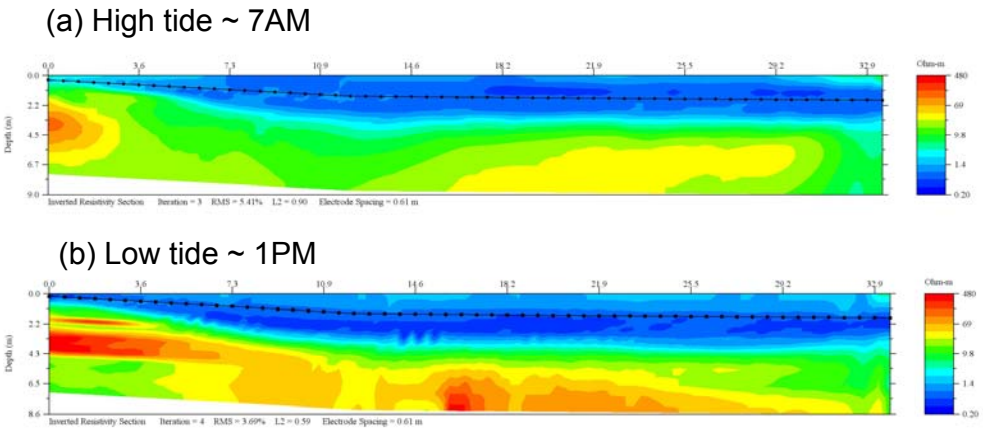

Figure 5: Transient transect FR2A of the West shore of Forge River. Date of acquisition: December 8th 2008 at high tide for (a) and low tide for (b).

4 Comparison of the Electrical Resistivity Inversion with Trident and Seepage Meter Data

Our Trident probe and seepage meter data provide complementary information on electrical resistivity and SGD, although they were acquired at different dates. Trident data were acquired on October 25 2007 at ~12pm which was half time from high tide towards low tide, near locations 2I and 2J marked in Figure 4. In Table 1 we compared the measured values with those inferred from inversion of the Supersting data in Figure 4. It can be seen that the Trident measurements are bracketed by inversion data using the two different approaches. In future work, we will conduct Trident and Supersting measurements simultaneously so that direct constraints can be placed on inversion of the electrical resistivity data.

Table 1: Comparison of the resistivities measured with the Trident probe and obtained by inversion with both given (a) and free (b) water resistivity. The Trident measured the resistivity in the sediments at a depth of 46cm.

Trident point	Sediment resistivity measurement (in ohm-m)	Sediment inverted resistivity From (4a) (in ohm-m)	Sediment inverted resistivity From (4b) (in ohm-m)
FR2S-2I	5.9	9.2	0.5
FR2S-2J	83.3	600	2

Ultrasonic seepage meters were deployed at station FR-2A from October 18 through October 29, 2007. Results for the funnel 1 for 24 hours at station FR-2A are shown in Figure 5. The maximum flow rate for funnel 1 at station FR2-A was 71.51 cm/d, the minimum was 1.24 cm/d and the average was 48.97 cm/d. The funnel 2 (not shown here) had a maximum flow rate of 103.54 cm/d, and a minimum of 0.95 cm/d and the average was 38.93 cm/d. Sediments at this station consist of mostly sand and coarse gravel accounting for relatively high flow rates compared to the two stations further offshore. A rain event occurred on the 19th that could account for high flow throughout the high tide on funnel 1.

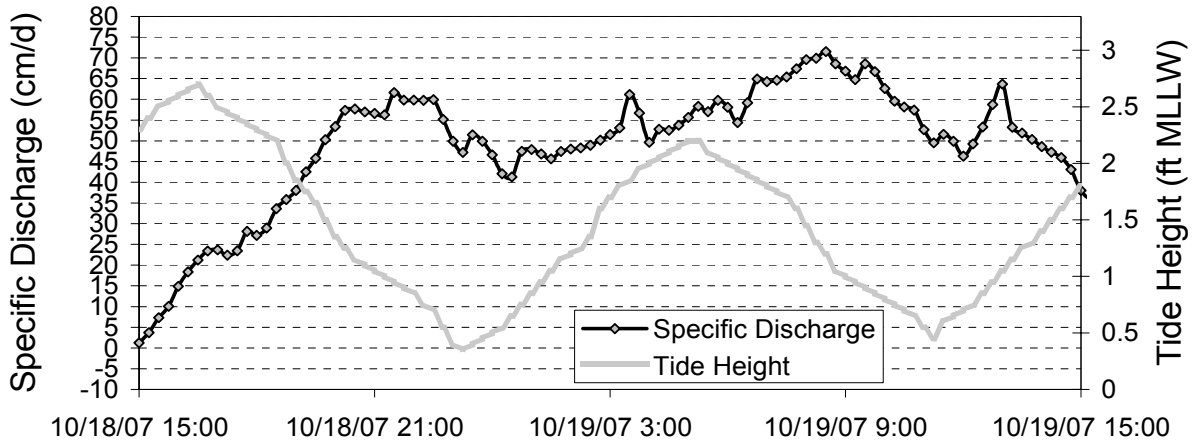

Figure 5 Ultrasonic seepage flow data for funnel 1 at station FR2-A

The measured values are comparable to the moderate SGD rates measured in other sites like Cockburn Sound, Australia: mean seepage rate of 32 cm/d or Shelter Island: 32.5cm/d at low tide and 5cm/d at high tide [*Stieglitz et al.*, 2008]. The anticorrelation between the tidal stage and SGD was not observed at our points of measurements. This indicates that the tidal loading is not the only controlling factor of pressure change in our system. The seepage meters confirm the presence of freshwater release seen as plumes on the electrical resistivity inverted section.

Conclusion

The three methods used in our study of Forge River yield results that are in good agreement with one another. The resistivity data from the Trident probe exhibit results close to the resistivity inverted section by one order of magnitude. This difference is attributed to the distinct season and tidal stages at which the measurements were made. The resistivity sections allowed us to identify a plume of freshwater (with resistivities up to 216 ohm-m) on the West shore of Forge River. The plume extends on 30 m towards the center of the river and its thickness varies from at least 8 m on the river bank to 4 m farther. It is consistent with the seepage measurements that give a mean rate of 39 cm/d. SGD is thus a potential nitrogen source in Forge River. Knowing the nitrogen species concentrations from water sample analysis should then allows to quantify the amount of nitrogen input from SGD into Forge River. Comparisons between sections at different tidal stages and different year show that the results are consistent, even if there are not directly constrained by the Trident data. As our sensitivity study demonstrated the importance of the adequate water depth, it is crucial to improve the accuracy of the comparison between methods to have the measurements made at the same tidal stage. We showed that the inversion is also greatly stabilized if the seawater resistivity is let as unknown during the inversion. It is then necessary to have independent electrical resistivity measurements to check the results. In future work, we will conduct Trident and Supersting measurements simultaneously so that direct constraints can be placed on inversion of the electrical resistivity data.

Acknowledgments

We thank Bradley Carr from AGI, for his help to deal with some instrumentation difficulties and his valuable inputs regarding the inversion process. The inversion analysis was partially supported by EPA's Peconic Estuary Program.

References

Aller, R. C., C. J. Gobler, and B. J. Brownawell (2009), Data report on benthic flux studies and the effect of organic matter remineralization in sediments on nitrogen and oxygen cycling in the Forge River, New York: Task #1 and 2. Prepared for Suffolk County Department of Health Services*Rep.*, 62 pp.

Chadwick, D. B., A. Gordon, J. Groves, C. Smith, R. Paulsen, and B. Harre (2003), New tools for monitoring coastal contaminant migration, *Sea technology*, *44*(6), 17-22.

Day-Lewis, F., E. White, C. Johnson, J. Lane Jr, and M. Belaval (2006), Continuous resistivity profiling to delineate submarine groundwater discharge--examples and limitations, *The Leading Edge*, *25*(6), 724.

Paulsen, R. J., C. F. Smith, D. O'Rourke, and T. F. Wong (2001), Development and evaluation of an ultrasonic ground water seepage meter, *Ground Water*, *39*(6), 904-911.

Paulsen, R. J., D. O'Rourke, C. F. Smith, and T. F. Wong (2004), Tidal Load and Salt Water Influences on Submarine Ground Water Discharge, *Ground Water*, *42*(7), 990-999.

Stieglitz, T., J. Rapaglia, and H. Bokuniewicz (2008), Estimation of submarine groundwater discharge from bulk ground electrical conductivity measurements, *Journal of Geophysical Research*, *113*(C8), C08007.

Swarzenski, P. W., and J. A. Izbicki (2009), Coastal groundwater dynamics off Santa Barbara, California: Combining geochemical tracers, electromagnetic seepmeters, and electrical resistivity, *Estuarine, Coastal and Shelf Science*, *83*(1), 77-89.

Swarzenski, P. W., F. W. Simonds, A. J. Paulson, S. Kruse, and C. Reich (2007), Geochemical and geophysical examination of submarine groundwater discharge and associated nutrient loading estimates into Lynch Cove, Hood Canal, WA, *Environmental Science & Technology*, *41*(20), 7022-7029.

Swarzenski, P. W., W. C. Burnett, W. J. Greenwood, B. Herut, R. Peterson, N. Dimova, Y. Shalem, Y. Yechieli, and Y. Weinstein (2006), Combined time-series resistivity and geochemical tracer techniques to examine submarine groundwater discharge at Dor Beach, Israel, *Geophysical Research Letters*, *33*(24).

Taniguchi, M. (2002), Tidal effects on submarine groundwater discharge into the ocean, *Geophysical Research Letters*, *29*(12).

Taniguchi, M., W. C. Burnett, C. F. Smith, R. J. Paulsen, D. O'Rourke, S. L. Krupa, and J. L. Christoff (2003), Spatial and temporal distributions of submarine groundwater discharge rates obtained from various types of seepage meters at a site in the Northeastern Gulf of Mexico, *Biogeochemistry*, *66*(1), 35-53.

Telford, W. M., L. Geldart, and R. E. Sheriff (1990), *Applied geophysics*, Cambridge Univ Pr.